

Alma Mater Studiorum Università di Bologna
Archivio istituzionale della ricerca

Ceramics from Samshvilde (Georgia): A pilot archaeometric study

This is the final peer-reviewed author's accepted manuscript (postprint) of the following publication:

Published Version:

Randazzo L., Gliozzo E., Ricca M., Rovella N., Berikashvili D., La Russa M. F. (2020). Ceramics from Samshvilde (Georgia): A pilot archaeometric study. JOURNAL OF ARCHAEOLOGICAL SCIENCE: REPORTS, 34, 1-15 [10.1016/j.jasrep.2020.102581].

Availability:

This version is available at: <https://hdl.handle.net/11585/916961> since: 2023-02-22

Published:

DOI: <http://doi.org/10.1016/j.jasrep.2020.102581>

Terms of use:

Some rights reserved. The terms and conditions for the reuse of this version of the manuscript are specified in the publishing policy. For all terms of use and more information see the publisher's website.

This item was downloaded from IRIS Università di Bologna (<https://cris.unibo.it/>).
When citing, please refer to the published version.

(Article begins on next page)

This is the final peer-reviewed accepted manuscript of:

Randazzo L.; Gliozzo E.; Ricca M.; Rovella N.; Berikashvili D.; La Russa M. F.:
Ceramics from Samshvilde (Georgia): A pilot archaeometric study

JOURNAL OF ARCHAEOLOGICAL SCIENCE: REPORTS VOL. 34 ISSN 2352-409X

DOI: 10.1016/j.jasrep.2020.102581

The final published version is available online at:

<https://dx.doi.org/10.1016/j.jasrep.2020.102581>

Terms of use:

Some rights reserved. The terms and conditions for the reuse of this version of the manuscript are specified in the publishing policy. For all terms of use and more information see the publisher's website.

This item was downloaded from IRIS Università di Bologna (<https://cris.unibo.it/>)

When citing, please refer to the published version.

CERAMICS FROM SAMSHVILDE (GEORGIA): A PILOT ARCHAEOMETRIC STUDY

Randazzo L.^{1a}, Gliozzo E.^{1a}, Ricca M.¹, Rovella N.^{1*}, Berikashvili D.², La Russa M.F.^{1,3}

¹Department of Biology, Ecology and Earth Sciences (DiBEST), University of Calabria, 87036 Arcavacata di Rende, Cosenza (Italy)

²Department of Archaeology, Anthropology and Art of the University of Georgia. Kostava st. 77a. 0171. Tbilisi (Georgia)

³Institute of Atmospheric Sciences and Climate, National Research Council, Via Gobetti 101, 40129 Bologna (Italy)

^aThese Authors contributed equally to this study.

*corresponding author: natalia.rovella@unical.it

ABSTRACT

This archaeometric study deals with seven samples of Prehistoric pottery and - for the first time in the framework of Georgian studies - thirteen samples of glazed medieval pottery. All specimens were found at Samshvilde, the most remarkable archaeological complex in southern Georgia, and are believed to represent the local production. Two further samples of clayey and sandy raw materials were taken near the site and used for compositional comparison. Various analytical techniques were used for the investigation: optical microscopy, scanning electron microscopy, electron microprobe analysis, X-ray diffraction and X-ray fluorescence. The results allowed a fairly complex scenario to be reconstructed, both in terms of raw materials exploitation and technological choice for productions. The raw materials can be all referred to a volcanic environment and find a direct correspondence with the geological settings of the territory of Samshvilde. The techniques proved to be particularly interesting in relation to glazed ceramics, in fact, the eleven glazes were characterised as alkali, low alkali – low lead, lead, high lead and tin-opacified mixed-alkaline lead glazes. The compositional comparisons extend from east to west and place these ceramics in the wider framework of Islamic productions.

Keywords: prehistoric pottery; medieval pottery; lead glaze; tin glaze; alkali glaze; Samshvilde; Georgia.

1. INTRODUCTION

Surrounded by all other Caucasian regions (Turkey, Armenia, Azerbaijan and Russia), Georgia holds a key position for the understanding of production and commercial dynamics within these territories and in relation with the Near East civilizations.

The few archaeometric studies available so far mainly concern lithic industry and metallurgy. Obsidian tools were the object of recent archaeological (Badalyan et al. 2004, Grigolia and Berikashvili 2018, Berikashvili and Coupal 2018, Sagona 2018) and archaeometric research programs (Chataigner and Gratuze 2014a-b, Biagi and Gratuze 2016, Biagi et al. 2017, Le Bourdonnec et al. 2012; La Russa et al. 2019). Conversely, the archaeometric literature on metal objects is less consistent and mostly older (Kavtaradze 1999, Schillinger 1999, Hauptmann and Klein 2009, Stöllner and Gambashidze 2014, Erb-Satullo 2018).

As far as Georgian ceramics is concerned, only prehistoric finds have been investigated so far by Trojsi et al. (2002) and Kibaroglu et al. (2009). The former Authors performed mineralogical and petrographic analyses on a collection of sixteen Early Bronze Age ceramic samples from the settlements of Koda (Figure 1 no. 1), Kiketi (Figure 1 no. 2), Medamgreis Gora (Figure 1 no. 3), Satkhe (Figure 1 no. 4) and Kvatskhelebi (Figure 1 no. 5). Kibaroglu et al. (2009) performed petrographic and geochemical analysis on twenty Middle Bronze, Late Bronze/Early Iron Age ceramic samples from the archaeological sites of Udabno I (Figure 1 no. 6) and Didi Gora (Figure 1 no. 7) and on thirty-one clay samples in both the Sagaredjo district (Tetrobiani, Petrepauli, Patardzeuli and Karchana; Figure 1 nos. 8-11) and the Alazani basin (Ichalto, Vardiskubani, Pona and Bodbizchevi; Figure 1 nos. 12-15). In both cases, the Authors claimed a local origin of their sample set. Excluding the research performed by Shaar et al. (2017) on the “Levantine Iron Age geomagnetic anomaly” in Georgian pottery, these are the only two archaeometric investigations carried out on Georgian ceramics. Given the small progress made in this field, the present research has to remain on a rather exploratory level. In fact, before being able to plan an in-depth research on a specific topic, it is necessary to achieve a preliminary knowledge of the ceramic classes that, on the basis of archaeological typology, have been recognised as local productions. In order to properly address this investigation, the archaeological site of Samshvilde demonstrated high potentialities, proved by the diachronic and heterogeneous character of its ceramic collection. The archaeometric investigation is thus aimed at providing both a characterisation of the main prehistoric and medieval ceramic types deemed of local production and, especially, a guidance for future studies.

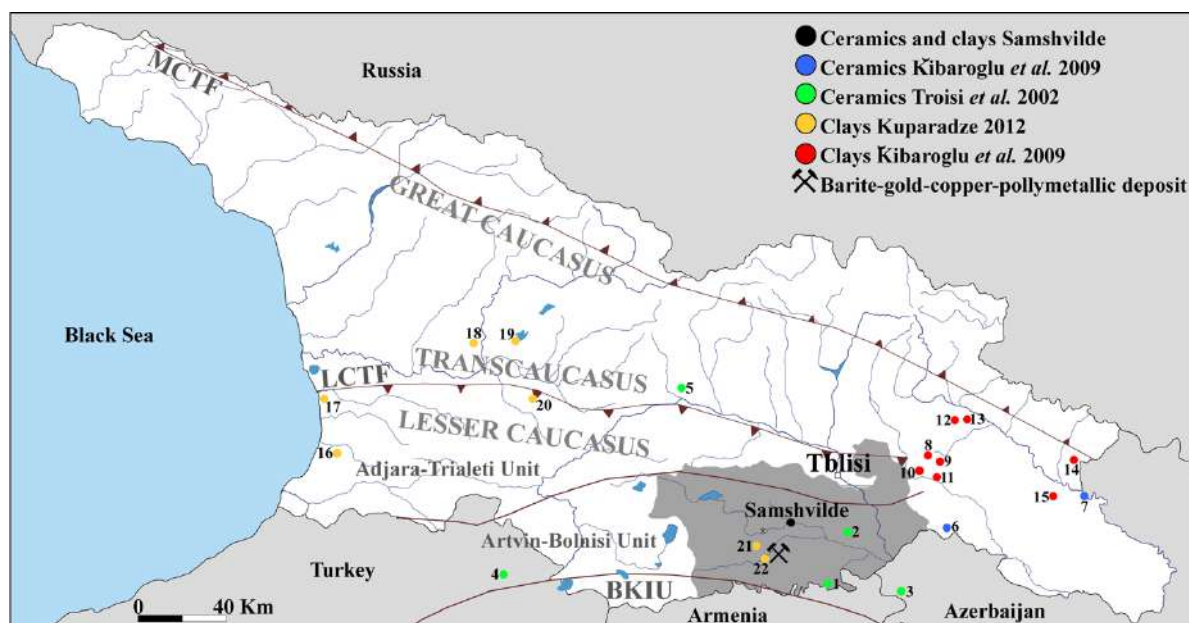


Figure 1. The geographical location of Samshvilde in Georgia. The divisions among the Adjara-Trialeti, Baiburt-Karabakh and Artvin-Bolnisi Units have been drawn after Yilmaz et al. (2000). The MCTF (Main Caucasus Thrust Fault) and the LCTF (Lesser Caucasus Thrust Fault) have been drawn after Sokhadze et al. (2018). Dark grey areas indicate the present Kvemo-Kartli administrative region. Sites that have been the object of previous researches: 1-Koda, 2-Kiketi, 3-Medamgreis Gora, 4-Satkhe and 5- Kvatskhelebi from Troisi et al. (2002); 6-Udabno I, 7-Didi Gora, 8-Tetrobiani, 9-Petrepauli, 10-Patardzeuli, 11-Karchana, 12-Ichalto, 13-Vardiskubani, 14-Pona and 15-Bodbizchevi from Kibaroglu et al. (2009); 16-Tsetsikhlauri, 17-Makvaneti, 18-Rioni, 19-Tkibuli, 20-Shrosha, 21-Darbazi and 22-Dambludi-Mashavera from Kuperadze et al. (2012). Clay samples nearby the site no. 19 have been further investigated by Bertolotti and Kuperadze (2018).

2. ARCHAEOLOGICAL BACKGROUND

Samshvilde is one of the most remarkable archaeological complex in southern Georgia and, overall, in the Caucasia territory (41°30'26"N, 44°30'20"E). The favourable geographical position was the main pull-factor that attracted people to the centre since the Stone Age. In fact, Samshvilde is located on a well defended promontory in the province of Kvemo Kartli, close to the southern branch of the Silk Road (Berikashvili and Coupal, 2018).

Seminal archaeological research projects were carried out during the Soviet period (Chilashvili 1970) while systematic investigations began in 2012, through the work of the University of Georgia. The current research program relies on an interdisciplinary base and it is aimed at improving our understanding of site development through the ages. During seven field seasons, the Neolithic, Bronze Age and Medieval phases were identified and materials recovered so far are the object of a combined archaeological and archaeometric study.

A brief overview of the main historical phases is provided below to help contextualise the on-going archaeometric research carried out on ceramics.

To begin with, the Middle-Late Bronze and Early Iron Ages are mainly testified by the high quantity of pottery found inside the citadel. In particular, a Late Bronze-Early Iron Age (13th-12th BC) burial (trench no. 68, nearly 5 meters below the ground surface; Berikashvili and Coupal, 2019) contained a cist and several fragments of black polished pottery, decorated with various geometric motifs (e.g. horizontal and vertical lines, zig-zag lines, concentric circles and inscribed notches). The most interesting find, however, was a large fragment of a jug with zoomorphic handle, representing a wild goat (*Capra aegagrus*) or a Caucasian tur (*Capra caucasicus*) with prominent horns.

The good state of conservation of the medieval contexts allowed for the research to be systematically explored. The political and economic role of Samshvilde became increasingly important from the 5th century AD and coincided with the increasing power of the Sasanian Empire in the South Caucasus. The dominance of the Sasanians lasted until the 7th century and then gave way to the rule of the Arabs. Since the mid 8th century (i.e. the foundation of the “Saamiro” of Tblisi), the Arab Emir governed a large part of the Kvemo Kartli region; however, the impact of the Arabic culture should have been minimal if one consider epigraphic documents such as the inscription on the East façade of the Cathedral where the Byzantine Emperors Constantine V and Leo IV are both mentioned.

From the mid-9th century onwards, the Shiraki Bagratuni royal dynasty reigned in Georgia and, in the 10th century AD, Samshvilde was referred to as the capital of the Tashir-Dzoraget Armenian Kingdom until the conquest of the Lore fortress by David IV and the consequent fall of the Tashir-Dzoraget Kingdom in 1118. The town reached its peak during the 12th century AD but the “golden age” ended abruptly with the arrival of the Mongols in the 1230s. Samshvilde became one of the main target areas and suffered a progressive decline, culminating with the Tamerlane’s raids (1400-1403) and the occupation by the Turkmen Shah Jahan (1440).

After the dismemberment of the Kingdom of Kartli in the 16th-17th centuries AD (Klimiashvili, 1964), the town experienced a new bloom in the mid-18th century, slightly before its definitive abandonment.

Based on the information provided above, it is clear that (a) Samshvilde is a complex and multicultural archaeological site with a diachronic unbroken continuity from the Neolithic to the 18th century AD and (b) its study is of paramount importance as source for the historical reconstruction of the entire Kvemo-Kartli region. The ceramic collection investigated here comes from the Samshvilde Citadel (Figure 2a) and the Sioni Area (Figure 2b).



Figure 2. Samshvilde Citadel from the East (a); the Sioni Cathedral and the excavated area.

The Citadel corresponds to the main fortification system of Samshvilde. Built of basalt boulders and mortar, consists of several building blocks (frequently restructured and repaired) arranged in a rectangular shape. Inside the walls, the remains of a large structure (the “palace”) are located in the northern area and a similar, larger structure (possibly a warehouse) has been found in the southern part. Between these two buildings, the baths were built, presumably, in the 16th-17th centuries AD (Berikashvili and Pataridze 2019).

Apart from the burial cist mentioned above, the archaeological excavation of the Citadel has brought to light numerous stone, ceramic, glass and metal objects dated back between the 5th and the 18th centuries AD (Berikashvili and Pataridze, 2019).

The area of Sioni is located in the eastern sector of Samshvilde and corresponds to the surroundings of the 8th century AD homonym Cathedral. The architectural style is that of the so-called transitional period and the archaeological excavations allowed for the recovery of obsidian and argillite tools (in the lower Neolithic layers) and a range of Bronze and Medieval pottery (in the upper layers; Berikashvili et al. 2019).

3. GEOLOGICAL SETTINGS OF THE KVEMO-KARTLI REGION

The archaeological site of Samshvilde is located in the central-east portion of the Artvin-Bolnisi tectonic zone, in turn bordered by the Adjara-Trialeti unit (Santonian-Campanian back-arc) at north and the Baiburt-Karabakh Imbricated unit at south (Upper Cretaceous fore-arc).

The Artvin-Bolnisi Unit is characterized by a Hercynian basement (Pre-Cambrian and Paleozoic granites-gneisses and S-type plagiogranites of the Khrami and Artvin Massifs), overlain by Carboniferous volcano-sedimentary rocks (Adamia et al. 2011). The Mesozoic is represented by volcanoclastic rocks of rhyolitic composition (Upper Triassic), overlain by terrigenous clastic sediments and limestones ('red ammonitic limestones'; Lower Jurassic) and Bajocian tuff-turbidites, lacustrine sandy-clays and lagoonal deposits (Upper Jurassic). The formation of conglomerates, sandstones, sands, shelf carbonate sediments took place in the Lower Cretaceous while calc-alkaline rocks, such as basalts, andesites, dacites and rhyolites were formed during the Upper Cretaceous.

Volcanic activity quieted down during the Late Senonian epoch and shallow-marine limestones and turbiditic terrigenous clastic sediments were deposited from the Palaeocene to the Lower Eocene. From the end of this period to the Late Eocene, volcanic activity resumed and a new series of calc-alkaline, subalkaline and alkaline volcanic rocks (andesites, shoshonites, basanites etc.) were erupted. The Upper Eocene is characterised by the deposition of shallow-marine clastic sediments while the succeeding orogenesis of the Caucasus (Oligocene) deeply modified the environment. The formation of the Great Caucasus, the Achara-Trialeti and the Lesser Caucasus mountains (in place of deep-water basins) resulted in both a sinking of the Georgian and Artvin-Bolnisi massifs and an accumulation of molasses in the depressions (until the Miocene). The last period of volcanic activity started in the late Miocene. In both the Lesser Caucasus and the Transcaucasus regions, (a) basaltic, dacitic, rhyolitic and, especially, andesitic lavas characterise the Upper Miocene–Lower Pliocene formations; (b) basaltic (doleritic) lavas are predominant in the lower part of the Upper Pliocene–Holocene formations and (c) andesites, andesite-dacites, and dacites represents the last volcanism (Lower Pliocene–Quaternary, maybe end of Pleistocene). These last rocks (no. 3 in Figure 3) are those upon which Samshvilde was built: a volcanic plateau overlooking the Khrami valley at south and those of the Chivchava valley at north.

The geomorphological studies performed by von Suchodoletz et al. (2016) on the Kura River and its tributaries (including the Khrami) have shown that rivers courses did not undergo significant channel migrations during the Quaternary. Moreover, the Authors provided some information on the heavy minerals content in the Khrami (sample HM-5; 41°28'21"N, 44°42'12"E) river: pyroxenes, amphiboles, mica, Ti-rich magnetite, tourmaline, sphene, apatite, olivine and epidote.

Georgian clays are poorly investigated. Excluding the clay deposits studied by Kibaroglu et al. (2009) and Bertolotti and Kuperadze (2018) that are very far distant from Samshvilde, only two samples have been investigated in the area of interest, at Darbazi and Dambludi-Mashavera (Kuperadze et al. 2012; sites nos. 21 and 22 in Figures 1 and 3). The Darbazi clays has been recognised as a weathering product of the Late Cretaceous acid volcanites and are associated to hydrothermally altered acid tuffs, trachytes and subvolcanic

bodies of rhyolites. Conversely, the Dambludi-Mashavera kaolinite-rich clays occur “as sheets on the old granites and alternate with quartz sandstones and conglomerates of Lower Lias”.

Lastly, the Bolnisi district deserves a mention because its gold and copper mines (Popkhadze et al. 2009) were exploited from the prehistory (esp. Sakdrisi; see Hauptmann and Klein 2009).

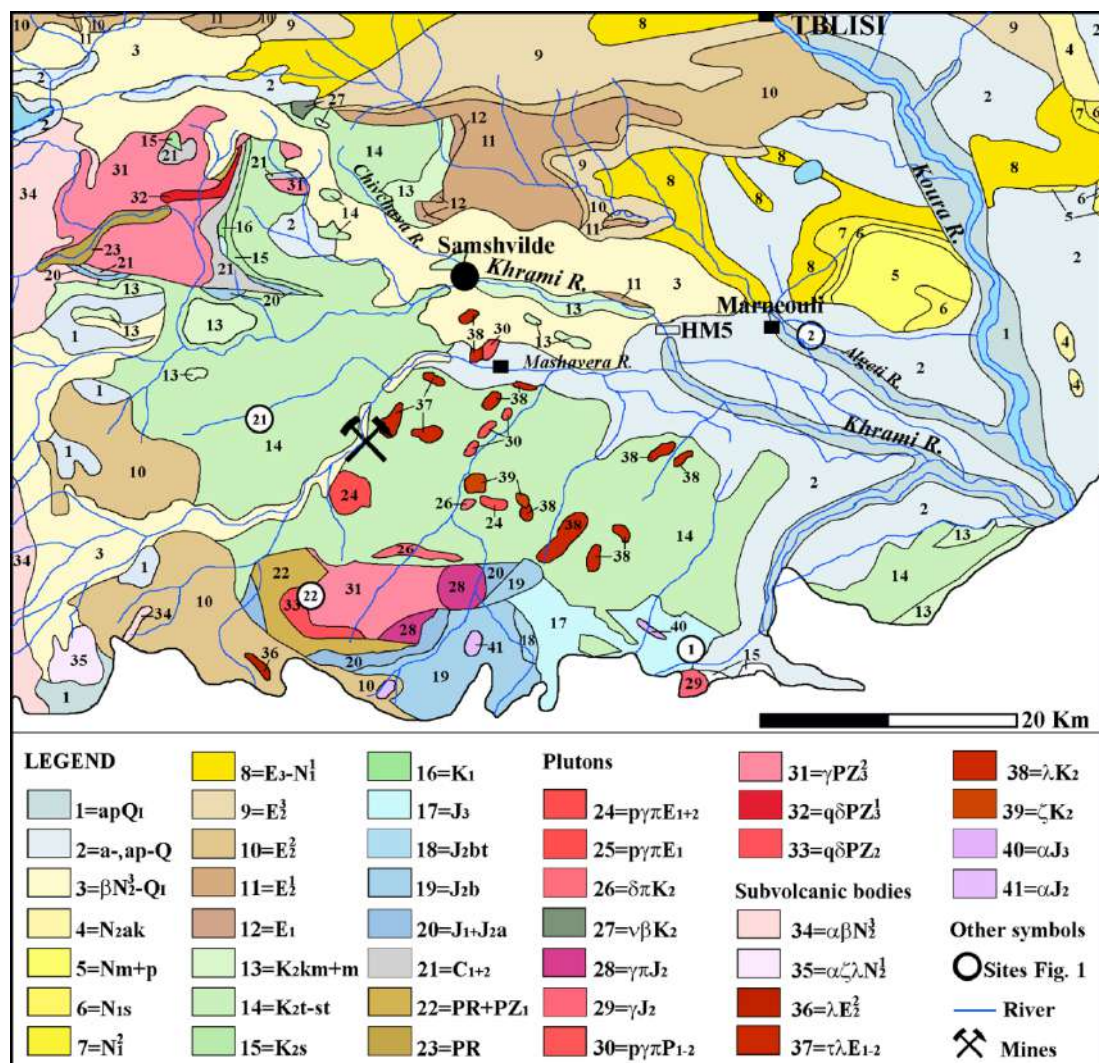


Figure 3. Geological map of the area of Samshvilde (simplified after Gamkrelidze and Gudjabidze 2003). The sites S1 and S2 (circled) correspond to Koda and Kiketi, respectively). The Legend is accurately reported in [Appendix 1](#). The description of nos. 3 and 13 is provided here because they outcrops in the territory of Samshvilde: 3) “Upper Pliocene-Lower Quaternary deposits. Lesser-Caucasian fold system: continental sub alkaline basalts, dolerites and andesite-basalts, andesites, lacustrine conglomerates, sands, sandstones, clays (Tsalka-Akhalkalaki suite)”); 13) “Campanian and Maastrichtian stages. Pelitomorphic limestones and marls, carbonate tuffites with intercalations of tuffs of dacitic composition”.

4. MATERIALS

Investigated samples include both local raw materials and ceramic fragments deemed of local production.

Raw materials. Two types of loose sediments were taken in the neighbourhood of the archaeological site of Samshvilde: 1) the samples KR2, that is representative of the clayey deposits outcropping near the

settlement, in contact with the alluvial dumps of Khrami River, and 2) the sample SAM 1, that is representative of sandy materials possibly used as tempers. Both samples were collected along fresh surfaces and soil covers were removed beforehand.

Ceramics. Both uncoated Late Bronze Age and glazed Medieval ceramics were selected for investigation. The former group of ceramics is poorly attested at Samshvilde, in fact, it was mainly found in the cist burial excavated inside the Citadel (trench no. 68). Bronze Age ceramics mainly include jars, jugs, bowls, plates and pots. Overall, the production is characterised by black polished surfaces, richly decorated with geometric motifs (e.g. horizontal and vertical lines, zig-zag lines, concentric circles and inscribed notches). Zoomorphic and round shaped handles are also common within black polished ceramics. This type of pottery is widespread in Eastern Georgia and several examples have been found at Meligele – I (Pitskhelauri, 1973; 2005), Dmanisi (Rezesidze, 2011), Tsiteli Gora (Abramishvili, 2008), Grakliani Gora (Kvirkvelia; Murvanidze, 2016) and Madnischalis Cemetery (Tushishvili, 1972). The seven samples investigated (Table 1, Figure 4) here were selected among pots, bowls and jars that are the most represented shapes.

The second group includes medieval glazed tableware and is representative of the typical Georgian ceramic production of the 11th -13th centuries AD. During this period -namely, the “Golden Age” in Georgia’s history- the country was unified under a central political government ruled by Monarch. This extended period of political stability favoured the development of several manufactures, especially that of pottery production. Surprisingly, unglazed pottery was produced to a lesser extent than the glazed one. Moreover, the distribution of Georgian glazed pottery crossed the national boundaries and became a characteristic commodity in neighboring territories such as present-day Azerbaijan, Armenia, Turkey and Iran. Indeed, glazed tableware was common in all this wide geographical area and the leading centers were located in Iran (especially, in northern Iran). Several centers such as Nishapur (Wilkinson, 1961), Mashhad, Tabriz and Ray (Wilkinson, 1973; Grube, 1976) were the leading centers; however, Georgia soon developed its own production, while remaining under the Iranian influence. Ceramic workshops producing glazed pottery have been found at Tbilisi (Chilashvili, 1999; Mindorashvili, 2009), Rustavi (Lomtadze, 1988), and Dmanisi (Djaparidze, 1956; Kopaliani, 1996). The thousands glazed artefacts recovered from the archaeological excavation of these sites revealed close typological and technical similarity and testified to a strong local traditions that lasted until the invasion of the Mongols (13th century AD).

The samples selected for this study were unearthed during the excavations of both the Citadel walls and the Sioni Area. The collections include glazed bowls, bearing colourful decorations typical of the 12th- and 13th centuries AD (table 1, Figure 4).



Figure 4. The investigated collection of prehistoric and medieval ceramics.

Table 1. Notable information on investigated ceramic samples and raw materials from Samshvilde. In column “Findsite”, localization and excavation data are reported (year of discovery in brackets). In column “shape”, which portion of the vessel was preserved is indicated in brackets.

Raw materials	Description and findsite				
KR 2	Clay deposit red-brown in color, Khrami river section. 41°30'23.76" N - 44°32'15.36"E				
SAM 1	Sandy deposit pale-yellow in color, close to the archaeological site. 41°30'51.48" N - 44°29'15.00"E				
LBA ceramics	Findsite	Ware	Type	Fragment	Chronology
ART 777	Citadel.Trench no. 68 (2018)	Black polished - with horizontal relief stripes	Bowl	Collar	13 th -12 th BC
ART 786	Citadel.Trench no. 68 (2018)	Fragment of reddish polished - with polished (vertically) and scratched (horizontally) stripes	Pot(?)	Wall	13 th -12 th BC
ART 791	Citadel.Trench no. 68 (2018)	Black polished with two deep horizontal scratched lines	Bowl	Rim	13 th -12 th BC
ART 799	Citadel.Trench no. 68 (2018)	Brownish polished	Pot(?)	Wall	13 th -12 th BC
ART 824	Citadel.Trench no. 68 (2018)	Black burnished ware	Jar	Wall	13 th -12 th BC
ART 831	Citadel.Trench no. 68 (2018)	Black cooking ware	Jar	Wall	13 th -12 th BC
ART 850	Citadel.Trench no. 68 (2018)	Black burnished ware with geometric motives	Bowl(?)	Wall	13 th -12 th BC
MA ceramics	Findsite		Type	Shape	Chronology
ART 6	Citadel. Trench#69 (2015)	Engobed-Glazed	Bowl	Base foot	12 th -13 th AD
ART 8Y	Sioni. Trench# N8 (2016)	Engobed-Glazed	Bowl	Wall	12 th -13 th AD
ART 8G	Sioni. Trench# O17 (2016)	Engobed-Glazed	Bowl	Wall	12 th -13 th AD

ART 12	Sioni. Trench# O17 (2016)	Engobed-Glazed	Bowl	Wall	12 th -13 th AD
ART 32	Sioni. Trench# N8 (2016)	Opaque glaze	Bowl	Wall	12 th -13 th AD
ART 34	Sioni. Trench# N8 (2016)	Engobed-Glazed	Bowl	Wall	12 th -13 th AD
ART 37	Sioni. Trench# N8 (2016)	Engobed-Glazed	Bowl	Wall	12 th -13 th AD
ART 42	Sioni. Trench# N8 (2016)	Engobed-Underglaze	Bowl	Wall	11 th -12 th AD
ART 76	Sioni. Trench# N8 (2016)	Engobed-Glazed	Bowl	Rim	11 th -12 th AD
ART 94	Sioni. Trench# O17 (2017)	Engobed-Overglaze	Bowl(?)	Rim	11 th -13 th AD
ART 170	Sioni. Trench# O17 (2017)	Engobed-Glazed	Bowl	Shoulder	12 th -13 th AD
ART 358	Citadel. Trench#60 (2017)	Engobed-Glazed	Bowl	Wall	11 th -12 th AD
ART 443	Sioni. Trench# O17 (2017)	Engobed-Underglaze	Bowl	Shoulder	12 th -13 th AD

5. EXPERIMENTAL

The analytical strategy was developed considering both the type of material under examination and the variable amounts of sample available for analysis. For this reason, the procedure and the analytical techniques used for the investigation of raw materials and ceramics are partially different and a selection of the samples to be submitted to each type of technique was necessary (see Supplementary Table 1).

Raw materials. Clayey raw materials were characterised in terms of textural (grain-size distribution) and compositional features (mineralogy and chemistry). Approximately 1 kg of each sample was air-dried, gently disaggregated, preliminarily homogenised and quartered. An aliquot of ca. 50 g of the quartered material was further dried in a laboratory oven at 60 °C for 48 hours and then left in the dryer to cool down to room temperature. This aliquot was mixed with de-ionised water and dispersed in an ultrasonic bath. The sand fraction was separated according to Stoke's law, dried in the oven (60 °C for 48 hours) and weighed. The remaining aqueous suspension containing the silt and the clay fractions was disaggregated in the ultrasonic bath. The silt fraction was separated in a centrifuge cycle at 2500 rpm, dried and weighed while the remaining (clay) fraction (particles measuring < 2 µm) was re-centrifuged at 4000 rpm for 10 minutes and submitted to X-ray diffraction and X-ray fluorescence analysis (the analytical conditions are specified below). For X-ray diffraction, a Bruker D8 Advance X-ray diffractometer (Bruker, Karlsruhe, Germany) with CuK α radiation, monochromated with a graphite sample monochromator at 40 kV and 40 mA was used. Scans were collected in the range of 3–60° 2 θ , 2° 2 θ min⁻¹ scan rate and 2s time constant. EVA software (DIFFRAC plus EVA version 11.0. rev. 0) was used for the identification of the mineral phases by comparing experimental patterns with 2005 PDF2 reference patterns. Semi-quantitative estimation was obtained on the basis of peak relative intensities. X-ray fluorescence was used to quantify major (SiO₂, TiO₂, Al₂O₃, Fe₂O₃, MnO, MgO, CaO, Na₂O, K₂O, P₂O₅) and trace elements (Ni, Cr, V, La, Ce, Co, Nb, Ba, Y, Sr, Zr, Zn, Rb, Pb) contents. The analyses were performed on pressed pellets made up of 5 g of specimen placed over boric acid (maximum working pressure 25 bar), through a Bruker S8 Tiger WD X-ray fluorescence spectrometer, with a rhodium tube with 4 kW intensity and an XRF beam of 34 mm.

Ceramics. For the preparation of the thin sections, the ceramic fragments were cut perpendicular to the surface of the artefact. All thin sections were investigated by optical microscopy (OM) and scanning electron microscopy (SEM-EDS). At the SEM-EDS, point analyses (5 µm beam diameter) on single phases and

square analyses (50/100 μm side) on the matrix were both carried out. Observations were mainly performed in back-scattered electrons. The instrument used was a Philips XL 30 SEM equipped with an Energy Dispersive Spectrometer (EDAX-DX4), working at 20 kV. A variety of natural silicates, oxides and synthetic materials were used as primary and quality control standards. Micro-chemical analyses were also carried out on the ceramic glazes, using an Electron Probe Micro Analysis (EPMA) JEOL-JXA 8230 coupled with 5 WDS Spectrometers XCE type equipped with a LDE, TAP, LIF and PETJ analyzing crystal. Working conditions were: 15 KeV HV; 10 nA probe current; 11 mm working distance; ZAF quant correction. A variety of mineral standards (jadeite, olivine, diopside, orthoclase, tugtupite, pyrite and galena) and pure metals (Fe, Ti, Mn, Cr, Cu, Zn and Sn) were used for calibration and quality control. Bulk chemical analyses were performed by X-ray fluorescence (XRF details are provided above).

The overall analytical strategy has been summarised in Supplementary Table 1.

6. RESULTS

Raw materials. Sample KR2 is characterised by a similar ratio of silt and clay, which are far more prevalent than the sandy fraction (Figure 5A). Based on Shepard's (1954), this sample can be classified as clayey silt (Figure 5B). Calcite and quartz were the main phases, followed by minor amounts of K-feldspar, plagioclase, pyroxene and clay minerals. Hematite showed weak peaks, slightly above the detection limit. The results provided by XRD agree with those obtained by XRF: the sum of SiO_2 , CaO and Al_2O_3 account for about the 85% of the total weight while the other oxides are present in minor amounts.

The sample SAM1, collected in the archaeological site, is characterised by a prevalent gravel fraction, followed by the sand, silt and clay fractions (in order of decreasing amounts) (Figure 5C). Shepard's (1954) ternary diagram allows this sample to be classified as a gravelly sediment (Figure 5D). In the sandy fraction, medium (0.25-0.5 mm), fine (0.125-0.25 mm) and very fine (0.06-0.125) grains prevail over the coarser (>0.5 mm) ones. The mineralogical assemblage of this sample (XRPD) includes quartz, feldspar, plagioclase, clay minerals and traces of calcite, in order of decreasing abundance. Accordingly, bulk chemistry shows high SiO_2 and, to a lesser extent, Al_2O_3 contents, together with minor contents of all the other oxides.

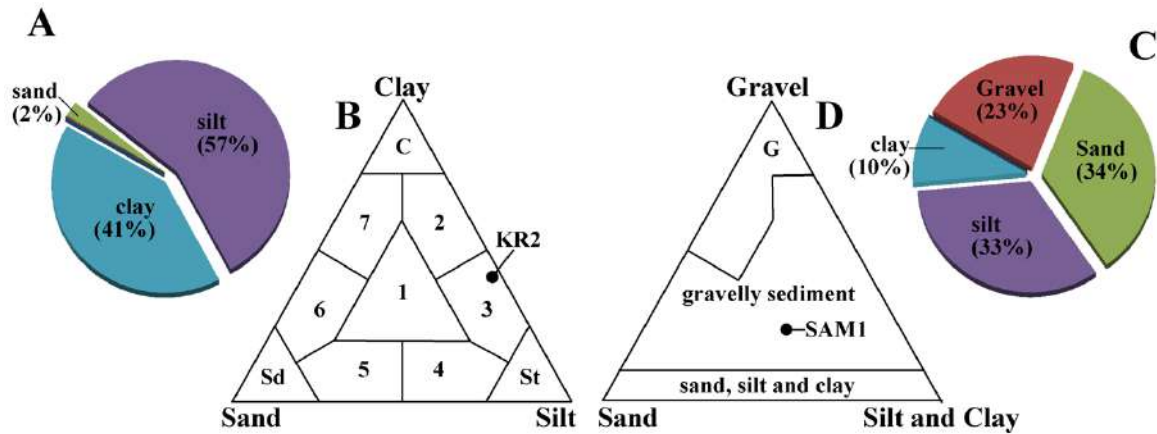


Figure 5. Grain size analysis on raw materials and the Shepard (1954) classification ternary diagrams for samples KR2 (A-B) and SAM1 (C-D). In ternary B: C=clay; St=silt; Sd=sand; 1) sand, silt and clay; 2) silty clay; 3) clayey silt; 4) sandy silt; 5) silty sand; 6) clayey sand; 7) sandy clay. In ternary D: G=gravel.

Ceramics. All samples show an unsorted serial texture. Five prehistoric ceramics (ART 791, 799, 824, 831, 850) and a medieval specimen (ART 94) show a coarse grain-size and porosity while all the others are characterised by a very fine grain-size and an extensive fine porosity. In three samples (ART 799, 824 and 850), the porosity has an elongated shape and a parallel orientation to the external surfaces.

The colour is homogeneous in samples ART 12, 32, 94, 358, 443 and 786 and unevenly distributed in the other samples: randomly zoned in ART 6, 170, 37, 42, 34, 8y, 8g, 76, 791 and 799 or core/surface zoned in ART 777, 824, 831 and 850.

Micro-textural features discriminate the fine grain-sized (i.e. mineral phases mostly ranging between 100 and 150 μm) samples ART 6, 8G, 8Y, 12, 32, 34, 37, 42, 76, 170, 358, 443, 777 and 786 from the coarse grain-sized (i.e. mineral phases mostly ranging between 150 and 250 μm) samples ART 94, 791, 799, 824 and 831. Both the roundness and the sphericity of the crystals are extremely variable while the high secondary porosity and the high sintering degree of ART 32 allow this sample to be distinguished from all the others.

The results obtained by bulk chemistry (Table 2) are in agreement with those obtained by SEM-EDS on the matrices (Table 3) and, on this basis, the collection can be divided into three main groups (Figure 6):

- 1) non-carbonatic ceramics (with CaO below 2.5 wt% and 1.4-3.6 wt% MgO), including 3 prehistoric (ART 786, 799 and 831) and one medieval sample (ART 32);
- 2) intermediate-carbonatic ceramics (with 6-10 wt% CaO and 3.2-3.9 wt% MgO), including two prehistoric (ART 791 and 824) and six medieval samples (ART 8G, 34, 8Y, 12, 443 and 42, in order of decreasing CaO contents);
- 3) carbonatic ceramics (with 11-14 wt% CaO and 3.3-4.7 wt% MgO), including one prehistoric (ART 777) and six medieval samples (ART 37, 6, 76, 170, 358 and 94, in order of decreasing CaO contents).

MgO contents are averagely around 3.5 wt% while much lower in ART 32 and much higher in ART 94, 358 and 777. The anomalous high lead contents revealed by several samples depends on the diffusion of this element from the glaze during firing, therefore, it cannot be considered as representative of the composition of the raw materials. Lastly, the high iron contents of samples ART 799 (Table 3) and ART 831 (Table 2 and 3) are also worth noting.

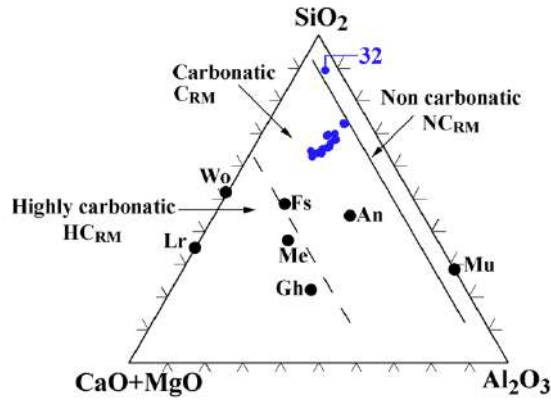


Figure 6. Ternary diagram illustrating the distinction between non-carbonatic, carbonatic and highly carbonatic ceramic bodies.

Table 2. XRF investigations on raw materials and ceramics. Values normalised to 100% without LOI.

Samples	SiO ₂ wt%	TiO ₂ wt%	Al ₂ O ₃ wt%	Fe ₂ O ₃ wt%	MnO wt%	MgO wt%	CaO wt%	Na ₂ O wt%	K ₂ O wt%	P ₂ O ₅ wt%	V ppm	Cr ppm	Co ppm	Ni ppm
KR2	51.66	0.75	13.84	6.59	0.12	4.60	19.15	0.73	2.41	0.15	178	89	20	67
SAM1	68.90	0.37	17.51	3.39	0.09	2.18	2.62	2.98	1.88	0.07	57	38	9	21
ART 6	56.66	0.77	15.57	7.58	0.13	3.64	10.90	2.34	2.09	0.29	153	99	22	53
ART 8G	56.90	0.86	16.28	8.50	0.12	4.20	8.13	2.74	2.03	0.16	181	102	27	48
ART 8Y	56.90	0.86	16.18	8.28	0.12	3.99	8.28	2.51	2.45	0.22	175	108	28	54
ART 34	57.04	0.83	16.44	8.28	0.12	4.07	8.29	2.38	2.26	0.29	191	97	27	53
ART 37	57.79	0.80	16.10	8.18	0.12	3.87	8.64	2.10	1.95	0.26	173	107	21	52
ART 42	57.85	0.78	15.83	7.92	0.13	3.81	8.87	2.35	1.94	0.31	158	104	26	55
ART 443	55.99	0.82	15.21	7.82	0.13	3.81	9.71	2.32	1.98	0.31	165	105	25	54
ART 831	60.85	0.96	17.00	9.22	0.14	4.45	3.33	1.67	2.16	0.22	186	146	27	83

Samples	Cu ppm	Zn ppm	As ppm	Rb ppm	Sr ppm	Y ppm	Zr ppm	Nb ppm	Sn ppm	Ba ppm	Pb ppm	La ppm	Ce ppm	LOI
KR2	39	105	-	121	401	32	151	16	22	321	36	17	52	20.7
SAM1	18	59	23	58	454	13	93	8	9	527	18	8	33	8.0
ART 6	87	99	14	69	458	30	158	13	-	460	180	17	44	3.1
ART 8G	149	99	-	69	488	30	157	13	12	433	799	31	47	2.6
ART 8Y	90	99	-	63	530	35	154	11	15	504	2018	25	39	2.0
ART 34	63	95	15	71	448	28	150	14	21	462	150	21	46	3.3
ART 37	78	98	5	66	440	29	157	14	12	461	2090	12	42	2.8

ART 42	74	96	-	70	499	27	145	11	-	563	2096	23	43	3.0
ART 443	123	99	-	83	562	30	173	12	21	522	18981	18	40	3.0
ART 831	43	111	15	69	273	33	178	13	-	703	24	33	58	7.7

Table 3. SEM-EDS (wt%) results on the fine matrix. A minimum of five measurements have been taken for each sample, using square analyses of 50/100 μm (side).

		SiO ₂	TiO ₂	Al ₂ O ₃	FeO	MnO	MgO	CaO	Na ₂ O	K ₂ O
ART 32	av.	82.8	0.9	7.0	0.7	0.1	1.4	1.7	4.1	1.3
	sd.	1.1	0.3	0.4	0.1	0.1	0.1	0.2	0.3	0.2
ART 799	av.	63.3	0.9	18.3	7.4	0.1	3.6	2.2	1.4	2.6
	sd.	0.9	0.1	0.5	0.3	0.1	0.3	0.1	0.2	0.0
ART 786	av.	63.1	1.0	18.2	6.1	0.4	3.1	2.3	2.3	3.6
	sd.	1.6	0.2	0.7	0.4	0.2	0.3	0.2	0.4	0.3
ART 831	av.	63.9	1.0	17.8	7.0	0.3	3.4	2.4	1.4	2.8
	sd.	0.8	0.2	0.6	0.3	0.2	0.2	0.4	0.3	0.1
ART 8g	av.	59.2	1.0	18.1	6.0	0.2	3.9	6.0	3.4	2.2
	sd.	0.6	0.3	0.7	0.6	0.2	0.2	0.9	0.2	0.3
ART 824	av.	60.7	1.1	17.2	6.2	0.3	3.5	6.0	1.6	3.3
	sd.	1.4	0.2	0.5	0.4	0.1	0.2	0.4	0.3	0.2
ART 34	av.	59.3	0.7	17.9	5.8	0.2	3.8	6.4	3.2	2.7
	sd.	1.0	0.1	0.7	0.4	0.1	0.4	0.4	0.3	0.3
ART 8y	av.	58.7	0.7	17.6	5.5	0.3	3.9	7.8	3.1	2.3
	sd.	2.4	0.2	1.0	0.9	0.1	0.7	0.9	0.2	0.3
ART 791	av.	61.0	0.8	15.9	6.2	0.2	3.2	7.9	1.6	3.1
	sd.	1.6	0.1	1.0	0.4	0.2	0.3	1.4	0.3	0.3
ART 12	av.	62.0	0.6	15.8	2.0	0.5	3.7	8.1	6.0	1.4
	sd.	6.0	0.3	1.7	1.1	0.3	0.8	2.1	0.7	0.2
ART 443	av.	58.0	0.6	17.9	5.5	0.2	3.5	9.1	3.0	2.0
	sd.	1.8	0.1	0.9	0.5	0.0	0.5	1.9	0.2	0.3
ART 42	av.	58.1	0.6	17.7	5.2	0.1	3.8	9.7	3.0	1.8
	sd.	1.6	0.3	0.6	0.4	0.1	0.4	1.7	0.2	0.1
ART 37	av.	56.6	1.7	16.5	6.0	0.3	3.3	10.9	2.5	2.0
	sd.	2.7	1.0	1.7	1.4	0.1	0.4	2.2	0.3	0.0
ART 6	av.	56.5	0.8	16.9	5.6	0.3	3.6	11.2	3.0	1.9
	sd.	3.0	0.4	0.6	0.8	0.1	0.4	1.9	0.3	0.5
ART 76	av.	56.5	0.8	17.0	5.3	0.3	3.8	11.3	2.8	1.9
	sd.	1.5	0.2	0.4	0.6	0.1	0.5	1.8	0.3	0.2
ART 170	av.	56.9	0.7	17.3	5.7	0.2	3.6	11.6	2.7	1.1
	sd.	2.9	0.3	1.1	1.1	0.1	0.6	1.5	0.3	0.2
ART 358	av.	55.9	0.9	15.9	5.6	0.3	4.0	11.8	2.9	2.4
	sd.	2.0	0.1	0.9	0.3	0.1	0.0	1.6	0.2	0.2
ART 94	av.	56.7	0.9	14.1	5.0	0.3	4.7	12.7	3.6	1.9
	sd.	2.8	0.1	0.5	0.5	0.1	0.7	1.7	0.9	0.5
ART 777	av.	56.3	0.8	15.4	5.0	0.3	4.2	13.8	2.0	2.1

The results of the mineralogical and petrographic investigations performed on ceramic bodies are presented first, separately from those obtained on glazes. The presence of quartz, K-feldspars and accessory minerals such as Fe and Ti oxides represents a common, non-discriminant feature. Among phyllosilicates, white mica has been rarely observed in samples ART 170, 791 and 799. Small Mg-Fe chlorites and small biotites (usually showing K-loss) have been sporadically found in all samples and, in both cases, they rarely exceeded 150 μm in length. More abundant and larger aggregates of chlorites have been observed in samples ART 786, 791, 799, 824 and 831.

The relative amount of the different plagioclases can be used to identify five groups of ceramic bodies: 1) samples with the entire series of plagioclases (from albite to anorthite) equally represented (ART 786 and 34); 2) samples with prevalent albite (ART 37 and 791), together with andesine (ART 831) or labradorite (ART 42, 799 and 824) or bytownite (ART 443); 3) samples with prevalent andesine (ART 12 and 94), together with bytownite (ART 170); 4) samples with prevalent labradorite (ART 6, 358, 777), together with bytownite (ART 8Y); and 5) samples with prevalent bytownite (ART 8G and 76).

Among carbonates, traces of dolomite have been found in ART 94 while calcite was (a) completely absent in samples ART 32, 799, 786 and 831 (either because originally absent in the raw materials or transformed by firing); (b) decomposed due to firing in ART 76, 170, 358 and 791; (c) sporadic, without clear traces of destabilization in ART 8G, 12, 34, 824 and 850; (d) sporadic, with thin reaction rims in ART 37, 42 and 443; (e) sporadic but almost decomposed in ART 8Y and 42; (f) frequent, without traces of destabilization in ART 777; (g) frequent, with evident traces of advanced decomposition in ART 6 and 94.

Among pyroxenes, while orthopyroxenes have been rarely found (enstatite/Mg-pigeonite in ART 6, 8G, 8Y, 34 and 831), clinopyroxenes are ubiquitous in all samples, except for ART 94 (Figure 7). Primary clinopyroxenes show an augitic (ART 6, 8Y, 37, 358, 791, 799, 824 and 831) or augitic and salitic (ART 8G, 12, 34, 76, 170, 443 and 777) or augitic and diopsidic (ART 32, 42 and 786) composition. Newly formed pyroxenes have been found in three samples: 1) ART 94, showing frequent skeletal rods of diopsidic pyroxene, confined in the interface between the ceramic body and the coating layer (below 15 μm); 2) ART 170, showing sporadic Al-rich clinopyroxene, rimming former calcite grains; and ART 358, showing sporadic Al-rich clinopyroxene, rimming ovoidal pores (likely of former microfauna).

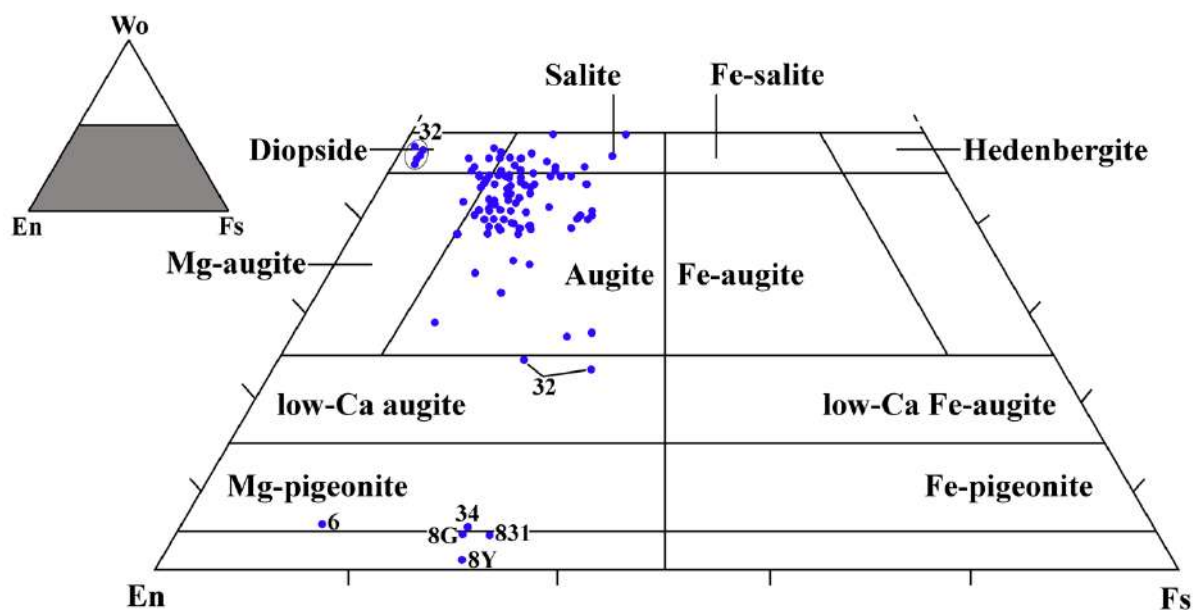


Figure 7. The chemical composition of the pyroxenes, plotted in the wollastonite (Wo), enstatite (En), ferrosilite (Fs) ternary diagram.

Amphiboles are ubiquitous but never abundant such as clinopyroxenes. Clinoamphibole with a brown colour and a Ti-rich hornblende composition have been found in samples ART 6, 8Y, 34, 37, 42, 358, 443 831 and 850. Other green clinoamphiboles, showing a slightly different composition (i.e. not Ti-rich), have been found in samples ART 6, 8G, 34, 94 and 443.

Table 4. The composition of glazes (Gl) and slips (Sl) measured by EMPA. Average (n=) and standard deviation (sd) values. [The slip of samples ART76 and 170 have been analysed by SEM-EDS]

Analysed by SEM EDS

ART	Colour	Area	n	SiO ₂	TiO ₂	Al ₂ O ₃	Cr ₂ O ₃	FeO	MnO	MgO	CaO	Na ₂ O	K ₂ O	Cl	SO ₃	ZnO	SnO ₂	CuO	PbO	Total
Alkali glazes																				
76	R	Gl	3	71.88	0.25	6.04	0.00	2.69	0.12	2.37	4.58	7.82	1.90	0.41	0.18	0.05	0.03	1.65	0.02	99.9
			sd	1.84	0.06	1.50	0.00	1.44	0.03	0.44	0.72	0.54	0.17	0.07	0.06	0.03	0.04	0.19	0.04	
			Sl	3	57.8	0.1	25.7	0.00	0.6	0.1	1.5	0.8	5.9	0.7	0.00	0.00	0.00	0.00	0.00	0.00
94	Bk	Gl	4	82.55	0.10	4.68	1.27	1.81	0.01	1.96	1.25	3.34	2.00	0.07	0.06	0.01	0.13	0.67	0.08	99.9
			sd	11.72	0.08	3.43	1.53	1.59	0.01	1.56	1.37	2.12	1.36	0.05	0.05	0.03	0.12	0.88	0.09	
	Bl	Gl	4	78.18	0.21	4.65	0.05	0.36	0.06	1.24	1.90	5.92	2.39	0.06	0.08	0.02	0.45	4.23	0.22	99.9
			sd	1.30	0.09	1.34	0.04	0.11	0.02	0.22	0.31	0.15	0.11	0.02	0.05	0.02	0.09	1.40	0.13	
Low-lead-(low) alkali glazes																				
6	Tq	Gl	4	75.73	0.20	3.16	0.01	0.70	0.04	1.22	3.94	5.63	1.56	0.07	0.17	0.06	0.01	2.10	5.40	100.0
			sd	0.38	0.13	0.34	0.02	0.11	0.02	0.03	0.12	0.14	0.14	0.02	0.09	0.09	0.01	0.06	0.23	
			Sl	1	65.52	0.09	23.01	0.02	0.30	0.01	0.61	0.00	7.18	3.18	0.03	0.05	0.00	0.00	0.00	0.00
358	G	Gl	3	64.32	0.20	3.06	0.02	1.02	2.01	1.53	5.58	3.20	2.04	0.26	0.00	0.05	0.29	2.02	14.41	100.0
			sd	1.51	0.10	1.10	0.02	0.61	0.13	0.19	1.41	0.29	0.08	0.13	0.00	0.06	0.09	0.40	1.16	
			Sl	1	62.74	0.06	21.73	0.00	1.23	0.01	0.04	4.73	7.31	1.79	0.00	0.13	0.03	0.00	0.02	0.20
Lead glazes																				
170	G	Gl	4	55.39	0.06	2.14	0.01	0.47	0.02	0.66	1.16	2.99	0.65	0.20	0.00	0.00	0.24	2.29	33.73	100.0
			sd	1.41	0.06	1.13	0.01	0.07	0.01	0.03	0.17	0.18	0.02	0.04	0.00	0.00	0.28	0.31	2.10	
			Sl	1	77.1	0.3	13.4	0.00	0.92	0.01	1.89	1.2	2.1	2.6	0.00	0.00	0.00	0.00	0.00	0.00
8Y	Y	Gl	6	36.54	0.39	8.25	0.01	4.60	0.05	1.47	4.36	1.03	1.51	0.03	0.00	0.02	0.03	0.22	41.49	100.0
			sd	2.05	0.18	0.44	0.01	1.14	0.02	0.59	1.61	0.11	0.29	0.02	0.00	0.04	0.04	0.07	3.54	
8G	G	Gl	3	38.25	0.27	5.44	0.01	0.79	0.01	0.64	2.88	0.56	0.99	0.03	0.00	0.14	0.06	1.99	47.94	99.9
			sd	0.94	0.03	0.45	0.02	0.09	0.02	0.08	0.13	0.05	0.09	0.02	0.00	0.04	0.04	0.15	1.18	
High lead glazes																				
443	Tr	Gl	5	31.20	0.19	5.71	0.01	0.89	0.02	0.57	1.71	0.41	1.04	0.01	0.00	0.03	0.03	0.25	57.92	100.0
			sd	0.57	0.10	0.09	0.02	0.06	0.01	0.02	0.06	0.03	0.02	0.01	0.00	0.05	0.03	0.04	0.43	
			Sl	1	45.98	0.21	16.02	0.00	1.39	0.05	1.64	4.37	1.25	3.88	0.00	0.00	0.07	0.00	0.09	25.06
37	G	Gl	3	24.11	0.09	6.40	0.00	1.02	0.05	0.60	2.83	0.45	0.86	0.02	0.00	0.20	0.41	1.64	61.33	100.0
			sd	0.60	0.08	0.26	0.00	0.25	0.03	0.06	0.17	0.01	0.07	0.02	0.00	0.17	0.01	0.25	0.49	
			Sl	1	53.49	0.09	15.33	0.03	0.70	0.00	0.30	1.01	2.10	6.33	0.02	0.00	0.03	0.03	0.81	19.74
42	Y	Gl	4	24.14	0.09	6.79	0.02	0.45	0.02	0.58	1.40	0.33	1.01	0.01	0.00	0.01	0.01	0.10	65.05	100.0
			sd	0.34	0.07	0.25	0.01	0.11	0.01	0.05	0.05	0.02	0.23	0.01	0.00	0.01	0.01	0.04	0.41	
Tin glaze																				
32	Bl	Gl ext	5	55.93	0.07	1.59	0.01	0.55	0.02	2.06	3.55	5.76	1.16	0.69	0.00	0.04	3.74	0.03	24.80	100.0
			sd	0.66	0.06	0.06	0.02	0.04	0.02	0.06	0.14	0.06	0.03	0.03	0.00	0.05	0.26	0.03	0.72	
			Gl int	1	78.10	0.32	9.45	0.03	1.13	0.00	0.90	0.65	4.76	2.50	0.44	0.10	0.02	0.01	0.00	1.60
94	Bright crystals		1	6.8	0.2	9.1	56.1	7.1	0.2	12.7	0.1	0.3	0.1	0.0	0.0	0.0	0.0	7.3	0.0	100.0

[Colours abbreviations: Bl=blue; Bk= blackish dark olive; G=green; l.=light; R=red; Tr=transparent; Tq=turquoise; Y=yellow; W=white.]

Minor phases are represented by small crystals of olivine, spinel and garnet. Olivine has been found in samples ART 6 (Fo₇₆ with n=1), 8G (range Fo₅₈₋₆₃ with n=2), 443 (Fo₃₄ with n=1), 777 (average Fo₄₁ with n=2), and 791 (Fo₄₃ with n=2). Al-rich Cr-spinel and garnet have been found in sample ART 76 and in samples ART 6 (Py₂₆Gr₃₈Sp₃₅Al₁ with n=1) and 791 (Py₁₀Gr₅₃Sp₃₇ with n=1), respectively. These last phases, however, were so small that their presence in other samples cannot be excluded.

Lastly, abundant accessory and opaque minerals such as Ti-Fe oxides and apatite and, less frequently, titanite, epidotes and zircon are common accessory phases.

Lithic fragments have been observed in all samples except for ART 32. Sedimentary and volcanic rocks are typically present in both fine and coarse ceramics. The first type, which is more frequent and shows greater dimensions than the latter, is represented by frequent mudstones, sporadic sandstone and rare ARF (only in ART 42) or chert (only in ART 34). The second type shows trachytic, ophitic and intersertal textures and rarely exceed 350 µm in fine grain-size ceramics. The associations are bytownite + augite (ART 8G, 76), bytownite + augite + olivine (ART 791, 824, 831), and labradorite + augite (ART 6, 42, 170, 777, 799), possibly related to basalts and dolerites; andesine + augite (ART 8Y, 12, 42, 443) related to andesites; quartz + andesine + hornblende (ART 94), possibly related to dacites; and quartz + K-feldspar + augite + minor chloritised biotite and albite (ART 34), likely related to rhyolites. Other associations, like albite + augite (ART 799) or andesine/labradorite + K-feldspar (ART 777) or quartz + K-feldspar + biotite (ART 358) or K-feldspar + augite (ART 170) can be variously identified but the texture of these fragments suggest that a volcanic origin would probably be more likely than a plutonic or a metamorphic one. Volcanic glass was clearly identified only in ART 8Y but it is reasonable to assume that its presence could be more extensive, in fact, the small dimensions and the possible transformations due to firing may have prevented a proper estimation. The contribution from a metamorphic environment may be hypothesised on the basis of the association orthoamphibole + garnet + chlorite observed in a small clast of ART 6. Lastly, microfauna has been individuated in ART 12 and hypothetically reconstructed in ART 358.

The composition of the eleven glazes (Figure 8) has been investigated by EMPA (Table 4). The results allowed 4 types of glazes to be distinguished, on the basis of alkaline fluxes (Na₂O+K₂O) and lead amounts: 1) alkali glazes, composed of silica and alkali oxides (ART 76 and 94); 2) low alkali – low lead glazes, with alkaline fluxes and lead contents ranging between ~5 and 7 wt% and 5 and 15 wt%, respectively (ART 6 and 358); 3) tin-opacified mixed-alkaline lead glaze, with tin, lead and alkaline fluxes content of about 4, 25 and 7 wt%, respectively (ART 32); 4) lead glazes, with alkaline fluxes below 5 wt% and lead contents ranging between 30 and 50 wt% (ART 170, 8Y and 8G); 5) high lead glazes, with alkaline fluxes below 2 wt% and lead contents above 50 wt% (ART 443, 37 and 42).

Alkali glazes (ART 76, 94). The glaze layer of the carbonatic sample ART 76 shows variable but generally small (50-80 µm) thickness and an iron- and copper-rich composition. It is applied over a clear slip that measures 100-180 µm (thickness) and shows high alumina and very low iron contents. The carbonatic sample ART 94 shows a double layer coating: a rather thick (120-180 µm thickness) blue layer covered by a

thin (60-120 μm thickness) blackish dark olive layer. The composition of the two layers is similar, except for the main chromophores: copper in the lower layer, chromium and iron in the upper one. The measurement performed by EMPA on a single bright crystal shows a non-stoichiometric Fe- and Cu-bearing magnesiochromite composition (Table 4). Low amounts (below 1 wt%) of both lead and tin have been also measured in both layers. At the interface between the glaze and the ceramic body, newly formed diopsidic pyroxenes (typically of 15 μm) have been frequently observed.

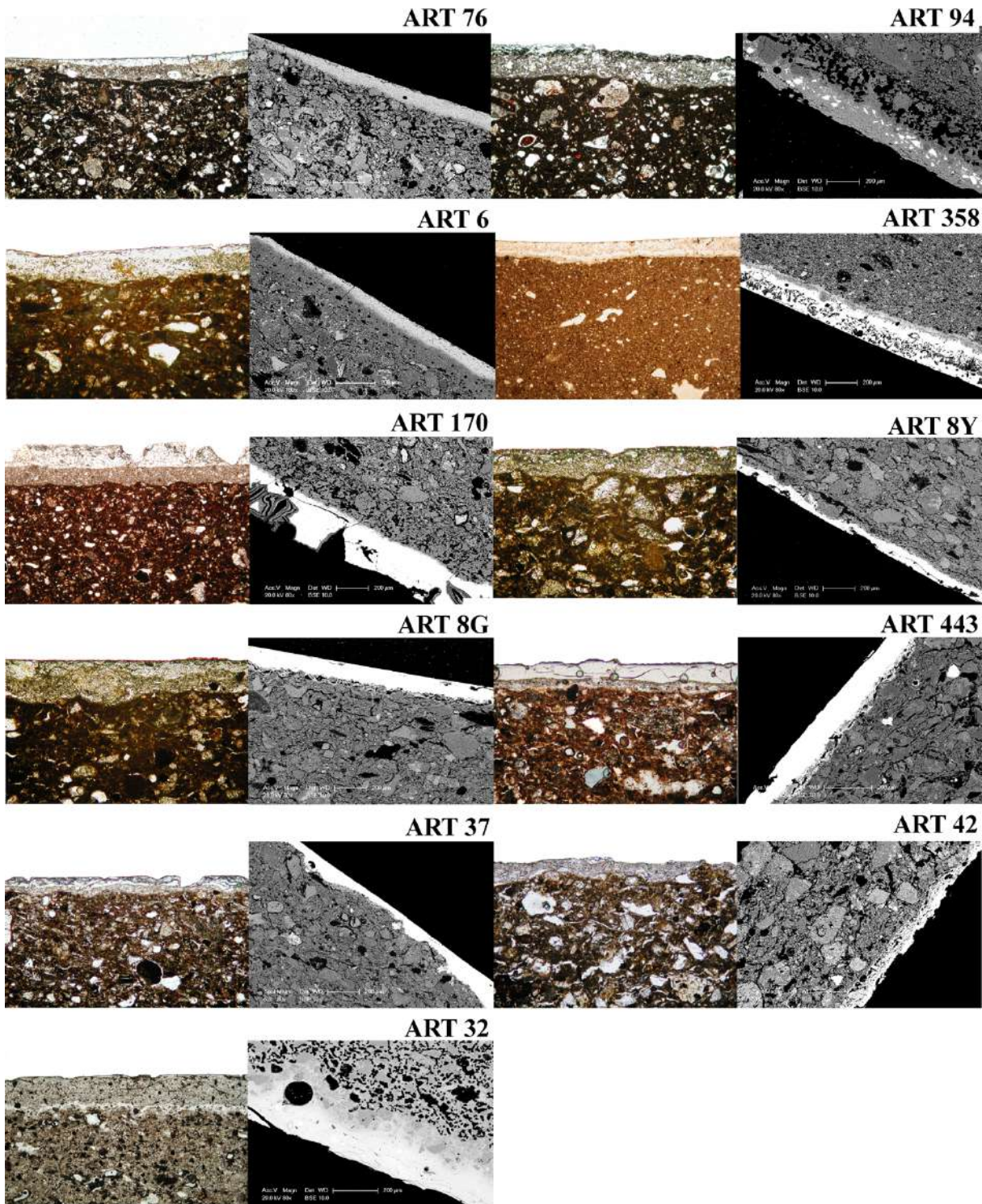


Figure 8. OM and SEM-BSE images of slips and glazes.

Low lead-low alkali glaze (ART 6, 358). The glaze of the carbonatic sample ART 6 contains high levels of copper and is applied over a creamy alumina-rich/iron-poor slip. The glaze of the calcareous sample ART 358 shows a regular and smooth profile, a thickness ranging between 120 and 200 μm and an advanced weathering characterised by notable alkali depletion. Apart from low lead amounts, this glaze also contains high contents of copper and manganese and very low tin amounts. With respect to the ceramic body, the thin (20-40 μm) slip at the interface with the glaze shows higher Al_2O_3 and Na_2O and lower SiO_2 , FeO , MgO , CaO and K_2O contents. Only a few crystals of quartz and, to a lesser extent, K-feldspar (both below 5 μm) can be observed in this slip.

Tin-opacified mixed-alkaline lead glaze (ART 32). In this sample, a layered glaze is applied over the ceramic body. The external portion shows a high thickness (up to 400 μm) and numerous, long and thin cracks; its homogeneous composition is made of alkali and lead, with small amounts of tin (ranging between 3.5 and 4.1 wt%) that confer a white opacity to the glaze (on the insolubility of tin particles in the lead glaze see Molera et al. 1999). Conversely, the internal interface is characterised by numerous crystals (up to 80/100 μm) of quartz embedded in a glassy layer, depleted in both Pb and Sn but Al- and Fe-rich than the upper one.

Lead glazes (ART 170, 8G, 8Y). The glaze of the calcareous sample ART 170 shows extensive cracking and heavy alteration. The thickness ranges between 180 and 250 μm and the composition is characterised by low levels of lead (~34 wt%), low levels of alkaline fluxes (below 4wt%) and high copper amounts. The slip is slightly thinner (150-220 μm) and highly porous. Its composition is Al- and Mg-rich than that of the glaze and Al- and Mg-poorer than that of the ceramic body).

The glazes of the intermediate carbonatic samples ART 8G and 8Y have similar thickness (30-180 μm in 8G, 40-150 μm in 8Y). ART8G shows a straight, smooth profile with small cracks unevenly distributed along the external 20-30 μm . ART 8Y shows an indented profile, frequent long cracks -especially parallel to the surface- and superficial alteration. In both samples, the glaze is applied on a discontinuous and very thin slip. The initial formation stage of the 'digestion' interface denotes a relatively low firing temperature (the digestion process is illustrated by Molera et al. 2001). The different colours are due to copper (green) and iron (yellow). In ART 8G, the association of high Zn and high Cu contents is notable.

High lead glazes (ART 443, 37, 42). The glaze of the intermediate carbonatic sample ART 443 shows a regular and smooth profile with a variable thickness (80-140 μm) and a composition characterised by small amounts of both copper and iron. The internal slip has variable thickness (20-80 μm) and its Fe-rich composition is partially contaminated by the upper lead glaze. The glaze of the carbonatic sample ART 37 has a variable thickness (50-250 μm) and a linear profile. The chromophore with the highest contents is copper and it can be likely associated with the relatively high contents measured for zinc and tin (both below 0.5 wt%). The slip is very thin (20-60 μm) and Fe-rich but, as similarly observed in ART 443, its composition is contaminated by the upper lead glaze. Lastly, the glaze of the intermediate carbonatic sample

ART 42 is poorly preserved. In the short traits where it is still visible it shows a very irregular thickness (40-90µm). The slip shows an irregular profile due to the poor smoothing of the ceramic body.

7. DISCUSSION

The main microstructural, chemical, mineralogical and petrographic features described in the previous section can be correlated to different raw materials and/or to different production technologies. The grain size, for example, clearly distinguishes fine wares from coarse wares and it likely addresses two different raw materials rather than a levigation process, since they are both poorly sorted. If the starting assumption is correct and these are local productions, this distinction could well correspond to diversified use of KR2-type clays, which may have been exclusive for fine wares and mixed with SAM1-type deposits for coarse wares. The content of carbonates provides a further distinctive criterion, since no temper made of spatic calcite has been observed. On this basis, non carbonatic, intermediate carbonatic and carbonatic ceramics should have used different raw materials; however, considering the typically high compositional variability of alluvial sediments, this reconstruction needs to be taken with caution. Combining the grain size with the non/carbonatic nature of the ceramic bodies, it is possible to divide fine and coarse wares on the basis of their carbonates content as shown in Table 5. On the same basis, a technological difference can be inferred, combining the degree of sintering of the matrix with the degree of transformation of calcite crystals. The general picture is complicated for fine ceramics because the maximum temperatures obtained during firing were low (i.e. low sintering degree and unreacted calcite), medium (i.e. low to medium sintering degree with calcite transformation in progress) and high (i.e. medium to high sintering degree and decomposed calcite), regardless of the amount of carbonates. Conversely, coarse wares were all low-fired, except for the Medieval sample ART 94. Given that the temperature range of calcite destabilisation and decomposition is of 650°-850°C, most samples were fired at maximum temperatures included in this range while a few samples, showing a higher sintering degree, no calcite and newly formed phases such as diopside and Al-rich clinopyroxenes (ART 94, 170, 358 and especially 32) reached maximum temperatures above 850°C.

Further information on production technology and use of these ceramics can be obtained from the observation of colour distribution and surface treatments. The samples ART 824 and 850, for instance, bore clear evidence of burnishing while samples ART 777 and 831 were used for cooking food on the fire. Moreover, the uneven distribution of colour in samples ART 6, 170, 37, 42, 34, 8y, 8g, 76 and 791 testifies for changing redox conditions during firing, given that compositional differences have not been observed between the brighter and darker areas. Conversely the homogeneous colour distribution of the other samples (especially ART 12, 32 and 358) suggests that a constant level of oxygen fugacity was maintained during firing or that an oxidising atmosphere was maintained for a sufficient time at the last stage of the process.

The composition of both plagioclases and primary pyroxenes combined with the mineralogical assemblages observed in lithic fragments provide a further hint as to where local materials were supplied. Among

plagioclases, for instance, sodic terms can be absent while calcic terms are ubiquitous and frequently combined with augitic clinopyroxenes, either as isolated crystals or as lithic fragments. The latter constantly refer to a volcanic environment, mainly represented by dolerites and andesites, although basalts, dacites and rhyolites can be also present. This evidence is consistent with the lithology of this area (see above the geological background) and therefore seems to support the local production of these ceramics. However, there are several features that suggest multiple production sites or multiple raw material supply sites, such as the partially different nature of the lithic fragments of sample ART 34, the presence of olivine in a few samples (ART 777, 6, 8G and 443), the abundant microfauna of sample ART12 and, possibly, the traces of former microfossils in ART 358.

As far as glazes are concerned, while the results obtained for the lead glazes are easily comparable within the broad framework offered by these types of ceramics, some interesting features emerged for the alkali glazes, the low alkali-low lead glazes and the tin glaze.

The alkali glazes (ART 76 and 94) have been applied on carbonatic bodies but the grain size is fine in ART 76 and coarse in ART 94. The use of a slip combined with an alkali glaze is not frequent but attested, for example, by the Islamic turquoise and blue '*coloured monochrome-glazed shards*' from Jordan investigated by al-Saad (2002) and the 12th-13th century AD alkaline glazes from Termez (Molera et al. 2020). Similarly, the overglaze technique showed by ART 94 has been identified in green and black 9th-10th cent. AD pottery from al-Andalus (Molera 2009, Molera 2013, Salinas 2018).

Continuing the comparison, the fluxing agents (soda and potash) and the alkaline earths (lime and magnesia) provide a small contribution to the glaze recipe in both samples (Table 5). These amounts testify to the use of plant ashes for lowering the melting temperature of this silica-rich glaze but make it difficult to compare these specimens with other alkaline glazes. The latter, in fact, are generally characterized by much higher alkali contents, for example, the sum of Na₂O and K₂O ranges between 16.7 and 19.3 wt% in Islamic pottery from Dohaleh in Jordan (al-Saad, 2002), between 11 and 16.7 wt% in 12th-17th century AD Termez productions (Molera et al. 2020), between 14 and 24 wt% and between 15 and 20 wt% in 11th-13th century Syrian and Iranian alkali glazes (Mason et al. 2001) or between 12.4 and 18.1 in 1st-7th century AD Sasanian glazed pottery from VehArdašīr (Pace et al. 2008).

As for colouring agents, while the comparison is straightforward for copper –i.e. a well-known and widely used chromophore, responsible for both the red (ART 76) and the blue (ART 94) colours- the use of chromium is more limited and likely began in a later period. Examples are provided by 9th-10th century lead glazes from Nishapur (Holakoei et al. 2019) and by 12th century black alkali-glazed from Iran (Mason et al. 2001).

The low lead-(low) alkali glazes (ART 6, 358) are both applied over an Al-rich slip, in turn applied over a carbonatic ceramic body. The particularity is the composition of the glaze that does not match with the compositional range provided by Tite et (1998) for the low lead-alkali type (2/10 wt% PbO, ~14 wt% Na₂O+K₂O, ~10 wt% MgO+CaO and 2 wt% Al₂O₃). ART 6 shows a lower amount of both fluxing agents

(~7wt%) and alkaline earths (~6 wt%) while ART 358 shows higher amounts of PbO and lower amounts of both fluxes (~5 wt%) and alkaline earths (~7wt%). Overall, these compositions find small comparison; for example, ART 6 can be compared with the Early Islamic Turquoise-glaze wares from Iraq investigated by Mason and Tite (1997; 1/3 wt% PbO, 9/20 wt% Na₂O+K₂O, 5/10 wt% MgO+CaO and 3/5 wt% Al₂O₃) while ART 358 finds a close comparison with green examples investigated by Henshaw (2010) from Uzbekistan (e.g. sample Tashkent 4). Conversely, colouring agents such as manganese (black strips of ART 358) and copper (turquoise and green) were commonly used.

The composition of the tin-opacified mixed-alkaline lead glaze (ART 32) is rather common (see e.g., Tite et al. 2008; Al-Saad, 2002; Gulmini et al. 2013, for comparison) but this specimen is particular because the glaze is applied over a non carbonatic high-fired ceramic body. For example, a few samples found at Termez (Uzbekistan; samples TA1 and TS1; Molera et al., 2020) show a similar composition but the glaze is applied over a carbonatic ceramic body. In this regard, it is also interesting to note that the reference materials are believed to be of Iraqi or Iranian or Syrian or, less probably, Egyptian provenance (Martínez Ferreras et al. 2019).

As noted above, lead glazes show techniques and compositions that can be considered as typical. Numerous similar examples are provided for pottery and tiles from Cyprus (Ting et al. 2019a), Jordan (Al-Saad 2002; Ting et al. 2019b), Egypt, the Levant, Mesopotamia, Iran and Central Asia (Matin et al. 2018 with tin), Afghanistan (Gulmini et al. 2013), Uzbekistan (Henshaw 2010 and Molera 2020), to central and western European countries such as Italy, Spain, Portugal and Britain (Tite et al. 1998; Coentro et al. 2017). The ceramic bodies are fine in grain size and intermediate-carbonatic to carbonatic in composition. In the glazes, Pb contents range between 34 and 65 wt% and the chromophores are represented by copper (turquoise in ART 170, green in ART 8G and 37) and iron (yellow in ART 8Y).

Lastly, in all samples (except for ART 42 and 170), the presence of low amounts of tin and/or zinc cannot be clearly related to an intentional addition while it may result from the introduction of brass or gunmetal as the source of copper.

Table 5. Results summary. Microstructural descriptions have been made on a comparative basis and they are relative to the examined context only. Detailed compositional data are provided in Tables 2-4 and Supplementary Table 2.

		Micro-structural features					Ceramic body									Glaze							
<i>Period</i>	<i>Sample</i>	Grain size	Roundness	Sphericity	Porosity	Sintering	Chemical c.	Calcite	Plagioclase	P. Cpx	N.F. Cpx	Cam	Minor	Lithic fr.	Microfauna	Colour	Slip	Type	Na ² O + K ² O	CaO + MgO	Pb	Sn	Chromop.
		<i>Fine</i>																					
LBA	ART 777	F	A/S	L/M	Hf	L	C _{RM}	Fu	La	Au/Sa	-	-	Ol	Ba-Do, V	-	-	-	-	-	-	-	-	-
MA	ART 6	F	S	L/M	Hf	L	C _{RM}	Fr	La	Au	-	B-G	Ol-Grt	Ba-Do;M?	-	T	X	1A-IPb	7	5	5	-	Cu
MA	ART 37	F	A/S	L	Hf	M	C _{RM}	Sr	Ab	Au	-	B	-	V	-	G	X	HPb	1	3	61	-	Cu
MA	ART 76	F	S/R	M/H	Hf	M	C _{RM}	D	By	Au/Sa	-	-	Cr	Ba-Do	-	R	X	A	10	7	-	-	Cu (Fe)
MA	ART 170	F	S/R	M/H	Hf	H	C _{RM}	D	An, By	Au/Sa	Al	-	-	Ba-Do, V	-	G	X	Pb	4	2	34	-	Cu
MA	ART 358	F	S/R	L/M	Hf	H	C _{RM}	D	La	Au	Al	B	-	V	?	G	X	1A-IPb	5	7	14	-	Cu-Mn
MA	ART 8Y	F	S	M	Hf	M	IC _{RM}	Sr	La, By	Au	-	B	-	An; G	-	Y	X	Pb	3	6	41	-	Fe
MA	ART 8G	F	A/S	L/M	Hf	M	IC _{RM}	Su	By	Au/Sa	-	G	Ol	Ba-Do	-	G	X	Pb	2	4	48	-	Cu
MA	ART 12	F	A/S	H	Hf	L	IC _{RM}	Su	An	Au/Sa	-	-	-	An	μF	G	X	n.a.	n.a.	n.a.	n.a.	n.a.	n.a.
MA	ART 34	F	A/S	L/M	Hf	L	IC _{RM}	Su	Ab/An	Au/Sa	-	B-G	-	Ry	-	-	X	n.a.	n.a.	n.a.	n.a.	n.a.	n.a.
MA	ART 42	F	A/S	L/H	Hf	M	IC _{RM}	Sr	Ab, La	Au/Di	-	B	-	Ba-Do, An	-	Y	X	HPb	1	2	65	-	-
MA	ART 443	F	A/S	L/H	Hf	M	IC _{RM}	Sr	Ab, By	Au/Sa	-	B-G	Ol	An	-	Tr.	X	HPb	1	2	58	-	Fe
MA	ART 32	F	A/S	-	Hs	vH	NC _{RM}	-	-	Au/Di	-	-	-	-	-	Bl	-	Sn	7	2	25	4	-
LBA	ART 786	F	A/S	L/M	Hf	L	NC _{RM}	-	Ab/An	Au/Di	-	-	-	V	-	-	-	-	-	-	-	-	-
		<i>Coarse</i>																					
MA	ART 94	C	A/S	L/M	Hc	M	C _{RM}	Fr	An	-	Di	G	-	Da	-	Bl-Bk	X	A	5	3	-	-	Cu-Cr
LBA	ART 791	C	A/S	L/M	Hc	L	IC _{RM}	D	Ab	Au	-	-	Ol-Grt	Ba-Do	-	-	-	-	-	-	-	-	-
LBA	ART 824	C	A/R	L/H	Hc	L	IC _{RM}	Su	Ab, La	Au	-	-	-	Ba-Do	-	-	-	-	-	-	-	-	-
LBA	ART 799	C	A/S	L/M	Hc	L	NC _{RM}	-	Ab, La	Au	-	-	-	Ba-Do, V	-	-	-	-	-	-	-	-	-
LBA	ART 831	C	A/R	L/H	Hc	L	NC _{RM}	-	Ab, An	Au	-	B	-	Ba-Do	-	-	-	-	-	-	-	-	-
LBA	ART 850	C	A/R	L/H	Hc	L	n.a.	Su	n.a.	n.a.	-	B	-	V	-	-	-	-	-	-	-	-	-

ABBREVIATIONS. **Microstructural features** - Grain size: F=Fine (with mineralogical phases averagely ranging between 100 and 150 μm); C=coarse (with mineralogical phases averagely ranging between 150 and 250 μm). Clasts roundness: A=angular, S=subrounded, R=rounded. Clasts sphericity: L=low, M=medium, H=high. Porosity: Hf =high fine; Hc=high coarse; Hs=extensive

secondary. Sintering degree: l=low, M=medium, H=high. Chemical composition (c.): NC_{RM}=non carbonatic raw material; IC_{RM}=intermediate-carbonatic raw material; C_{RM}=carbonatic raw material. **Mineralogical composition** - Prevalent plagioclases: Ab=albite; Ol=oligoclase; An=andesine; La=labradorite; By=Bytownite; An=anorthite. Calcite: D=decomposed; Su=sporadic and apparently unreacted; Ss=sporadic and slightly reacted; Sr=sporadic and reacted; Fu=frequent and unreacted; Fu=frequent and reacted. Primary (P) and newly formed (N.F.) clinopyroxenes (Cpx): Au=augite; Sa=salite; Di=diopside; Al=Al-rich clinopyroxene. Clinoamphiboles (Cam): B=brown hornblende; G=green hornblende. Minor (phases): Ol=olivine; Cr=Al-rich Cr spinel; Grt=garnet. Lithic fragments: Ba=basalt; Do=dolerite; An=andesite; Da=dacite; Ry=Rhyolite; V=generic volcanic; G=glass; M=metamorphic. Microfauna: μ F=frequent; ?=hypothetically present before firing. **Glazes** – Colour: Bl=blue; Bk= blackish dark olive; G=green; O=orange; R=red; T=turquoise; Tr.=transparent; Y=yellow; W=white. Glaze type: A=alkali glaze; lA-lPb=low alkali-low lead glaze; Sn= Tin-opacified mixed-alkaline lead glaze. In all fields n.a.=not analysed.

8. CONCLUSIONS

Taking up the history of archaeometric studies outlined at the beginning of this paper, it is clear that the research so far performed can be considered preliminary, particularly in consideration of the fact that it is mostly focused on prehistoric productions. In this framework, the research carried out on Samshvilde pottery has the merit of having presented, for the first time, the extreme variety and complexity of the medieval repertoire.

The analytical results describe a complex and heterogeneous ceramic collection, whatever the point of view from which it is observed. While such an outcome was expected as a consequence of a heterogeneous samples selection, several unexpected findings signal the need for additional studies and become new guidelines for future in-depth research.

The glazes, for instance, have proved to be compositionally different, in fact, their composition can be classified under the known types of alkali, low alkali – low lead, lead, high lead and tin-opacified mixed-alkaline lead glazes. Ground for comparison for lead glazes widespread from the Near East to the western Mediterranean basin while the composition and technique of alkali and low alkali – low lead partially differ from those provided by the literature and further particularities have been found in relation to the application of both an alkaline glaze over a coarse ware (ART 94) and a tin-opacified mixed-alkaline lead glaze over a non carbonatic ceramic body. In all cases, however, the differences (or the particularities) are never so sharp as to claim new productions but sufficient to underscore that these –poorly known- contexts can well contribute to the history of glazed ceramics, especially in the period medieval.

As for the localisation of the productions, the lack of reference groups weighs heavily on the conclusions we can draw. While the territory can be unique at a regional scale, the results do not suggest indicating Samshvilde -or another site included in the same area- as the only supply/production centre. The mineralogical assemblage and the lithic fragments can be referred to a volcanic environment but the extension of this environment cannot be further delimited. Assuming that prehistoric ceramics did not travel for long-range traits, the similarity of the petrographic results obtained for the prehistoric and the medieval pottery may indicate a limited geographic area; on the contrary, other features such as the carbonate contents, the presence/absence of specific phases (e.g. plagioclases and olivine) or microfauna, together with the compositional and technological differences observed in the glazes, seem to indicate a multiplicity of supply areas and production centres. Considering the glazes, for example, a provenance from other near eastern countries such as Iraq can be hypothesised for sample ART 32.

References

- Abramishvili, R., Abramishvili, M. 2008. Late Bronze Age Barrows at Tsitelgori, Archaeology in Southern Caucasus: Perspectives from Georgia, Ancient Near Eastern Studies, Supplement XIX, edited by Sagona and M. Abramishvili, Leuven- ParisDudley.
- Adamia, S., Zakariadze, G., Chkhotua, T., Sadradze, N., Tsereteli, N., Chabukiani, A., Gventsadze, A. 2011. Geology of the Caucasus: A Review. *Turkish Journal of Earth Sciences* **20**: 489–544
- al-Saad, Z. (2002) Chemical composition and manufacturing technology of a collection of various types of Islamic glazes excavated from Jordan. *Journal of Archaeological Science* **29**: 803-810. DOI: 0.1006/jasc.2000.0576
- Badalyan, R.S., Chataigner, C., Kohl, P. 2004. Trans-Caucasian obsidian: the exploitation of the sources and their distribution. In: A. Sagona (ed.), *A view from the highlands. Archaeological studies in honour of C. Burney*, Ancient Near Eastern Studies 12: 437–65. Leuven: Peeters.
- Berikashvili, D., Coupal, I. 2018. The First Evidence of Burials from Samshvilde A Preliminary Archaeological and Bioarchaeological Study. Caucasus Journal of Social Sciences. Vol. 11. The Publishing House of the University of Georgia. Tbilisi, pp. 31-49. <https://www.ug.edu.ge/storage/journals/January2020/dVSSYQjKu05dWbzYnyw7.pdf>
- Berikashvili D., Coupal Is., Tvaladze Sh., Kvakhadze L. 2019. The results of archaeological excavations in Samshvilde in 2019. Tbilisi.
- Berikashvili, D., Coupal, I. 2019. Recently Discovered Late Bronze Period Burial from Samshvilde Citadel. *Archaeology*, vol.3. The publishing house of the University of Georgia. Tbilisi, pp. 120-136.
- Berikashvili D., Pataridze M. 2019. *Samshvilde Hoard*. Tbilisi.
- Bertolotti, G.P., Kuparadze, D. 2018. White Firing Clays from Western Georgia. *Interceram* **67**:10-19.
- Biagi, P., Gratuze, B. 2016. New data on source characterization and exploitation of obsidian from the Chikiani area (Georgia). *Eurasiatica* 6: 9–35. DOI: 10.14277/6969-093-8/EUR-6-1
- Biagi, P., Nisbet, R., Gratuze, B. 2017. Discovery of obsidian mines on Mount Chikiani in the Lesser Caucasus of Georgia. *Antiquity* **91**(357): 1-8. DOI: 10.15184/aqy.2017.39
- Chataigner, C., Gratuze, B. 2014a. New data on the exploitation of obsidian in the southern Caucasus (Armenia, Georgia) and Eastern Turkey, Part 1: source characterization. *Archaeometry* **56**(1):25-47. DOI: 10.1111/arcm.12006
- Chataigner, C., Gratuze, B. 2014b. New data on the exploitation of obsidian in the southern Caucasus (Armenia, Georgia) and Eastern Turkey, Part 2: obsidian procurement from the Upper Palaeolithic to the Late Bronze Age. *Archaeometry* **56**(1):48-69. DOI:10.1111/arcm.12007.
- Chilashvili, L. 1970. ქალაქები ფეოდალურ საქართველოში II. [The cities in Feudal Georgia. Vol. II.] Tbilisi. [in Georgian]
- Chilashvili, L. 1999. თბილისის კერამიკული სახელოსნოს დაწგრევის თარიღისათვის სსმ. [For the dating of ceramic production center of Tbilisi]. Tbilisi. [in Georgian]

- Coentro, S., Alves, L.C., Relvas, C., Ferreira, T., Mirão, J., Molera, J., Pradell, T., Trindade, R.A.A., Da Silva, R.C., Muralha, V.S.F. 2017. The glaze technology of Hispano-Moresque ceramic tiles: a comparison between Portuguese and Spanish collections. *Archaeometry* **59**(4): 667-684. DOI: 10.1111/arc.12280
- Erb-Satullo, N. 2018. Patterns of settlement and metallurgy in Late Bronze–Early Iron Age KvemoKartli, Southern Georgia. In: Anderson, W., Hopper, K., Robinson, A. (eds.), *Landscape Archaeology in Southern Caucasia. Finding Common Ground in Diverse Environments*, Proceedings of the workshop held at 10th ICAANE (Vienna, April 2016), Austrian Academy of Science Press, pp.37-52.
- Gamkrelidze, I., Gudjabadze, G.E. 2003. *Geological map of Georgia. Scale 1:500.000*. Georgian State Department of Geology and national Oil Company Saqnavtobi"
- Grigolia, G., Berikashvili, D. 2018. Samshvilde Neolithic Stone Industry. *Archaeology*, vol.2. Tbilisi: The publishing house of the University of Georgia, pp. 87-108
- Grube, E. 1976. Islamic Pottery of the Eight-to the Fifteenth century in the Keir Collection. London.
- Gulmini, M., Giannini, R., Lega, A.M., Manna, G., Mirti, P. 2013. Technology of production of Ghaznavid glazed pottery from bust and Lashkar-i Bazar (Afghanistan). *Archaeometry***55**(4): 569-590. DOI: 10.1111/j.1475-4754.2012.00703.x
- Djaparidze, V. 1956. ქართული კერამიკა (XI-XIII სს.). [Georgian Ceramics. XI-XIIIcc.A.D.). Tbilisi. [in Georgian].
- Hauptmann, A., Klein, S. 2009. Bronze Age gold in Southern Georgia. *Revue d'archéométrie* 33:75-82. DOI: 10.4000/archeosciences.2037
- Henshaw, C.M.2010. Early Islamic ceramics and glazes of Akhsiket, Uzbekistan. Doctoral thesis, UCL (University College London).
- Holakooei, P., de Lapérouse, J.F., Carò, F., Röhrs, S., Franke, U., Müller-Wiener, M., Reiche, I. 2019. Non-invasive scientific studies on the provenance and technology of early Islamic ceramics from Afrasiyab and Nishapur. *Journal of Archaeological Science: Reports* **24**: 759-772. DOI: 10.1016/j.jasrep.2019.02.029
- Japaridze, V. 1956. Georgian Ceramic (XI-XIII cc.A.D.). Tbilisi.
- Kavtaradze, G.L. 1999. The importance of metallurgical data for the formation of a Central Transcaucasian chronology. In Hauptmann, A., Pernicka, E., Rehren, Th., Yalçin, Ü. (eds.), *The Beginnings of Metallurgy*, Der Anschnitt, Beiheft 9, pp. 67-101.
- Kibaroglu, M., Satir, M. and Kastl, G. 2009. Petrographic and geochemical analysis on the provenance of the Middle Bronze and Late Bronze/Early Iron Age ceramics from Didi Gora and Udabno I, Eastern Georgia. *Journal of Archaeological Science* **36**:2463-2474.DOI: 10.1016/j.jas.2009.07.005
- Klimiashvili, A. 1964. Materials for the history of Kartli and Kakheti administrative units in the 15-18th centuries. Collection: "Several Georgian historic documents of the 15-18th centuries". Tbilisi, pp. 122-123.
- Kopaliani, J. 1996. დმანისის ციხე. [Dmanisi Fortress (historical and archaeological research). Tbilisi: Sakartvelo publishers, 1996] Tbilisi. [in Georgian].

- Kuparadze, D., Pataridze, D., Bertolotti, G.P. 2012. Clays of Georgia for ceramic applications. *Interceram* 61: 178–183.
- Kutateladze, K. 2001. *Kvemo Kartli. Issues of Political History*. Tbilisi, pp. 68.
- Kvirkvelia, G., Murvanidze B. 2016. Archaeological Excavations at Grakliani Hill in 2011. Burial mounds of Bronze Period. *Dziebani*. #23. Tbilisi (in Georgian)
- La Russa, M.F., Randazzo, L., Ricca, M., Rovella, N., Barca, D., Ruffolo, S.A., Berikashvili, D., Kvakhadze, L. 2019. The first archaeometric characterization of obsidian artifacts from the archaeological site of Samshilde (South Georgia, Caucasus). *Archaeological and Anthropological Sciences* 11: 6725–6736. DOI:10.1007/s12520-019-00936-y
- Le Bourdonnec, F.X., Nomade, S., Poupeau, G., Guillou, H., Tushabramishvili, N., Moncel, M.-H., Pleurdeau, D., Agapishvili, T., Voinchet, P., Mgeladze, A., Lordkipanidze, D. 2012. Multiple origins of Bondi Cave and Ortvale Klde (NW Georgia) obsidians and human mobility in Transcaucasia during the Middle and Upper Palaeolithic. *Journal of Archaeological Science* 39: 1317–30. DOI: 10.1016/j.jas.2011.12.008
- Lomtadidze, G. 1988. ქალაქი რუსთავი არქეოლოგიური ძეგლების მიხედვით. არქეოლოგიური გათხრები 1946–1965. [Town of Rustavi according to archaeological sites. Archaeological excavations in 1946–1965]. Tbilisi. [in Georgian].
- Martínez Ferreras, V., Fusaro, A., GurtEsparraguera, J.M., Ariño Gil, E., Pidaev, S.R., Angourakis, A. (2019) The Islamic ancient Termez through the lens of ceramics: A new archaeological and archaeometric study. *Iran*. DOI: 10.1080/05786967.2019.1572430
- Mason, R.B., Tite, M.S. 1997. The beginnings of tin opacification of pottery glazes. *Archaeometry* 39(1): 41-58. DOI: 10.1111/j.1475-4754.1997.tb00789.x
- Mason, R.B., Tite, M.S., Paynter, S., Salter, C. 2001. Advances in polychrome ceramics in the Islamic world of the 12th century AD. *Archaeometry* 43(2): 191-209. DOI: 10.1111/1475-4754.00014
- Mindorashvili, D. 2009. არქეოლოგიური გათხრები ძველ თბილისში. [Archaeological Excavations in old Tbilisi]. Tbilisi. [in Georgian].
- Matin, M. (2018) On the origins of tin-opacified ceramic glazes: New evidence from early Islamic Egypt, the Levant, Mesopotamia, Iran, and Central Asia. *Journal of Archaeological Science* 97: 42-66. DOI: 10.1016/j.jas.2018.06.011
- Molera, J., Pradell, T., Salvadó, N., Vendrell-Saz, M. 1999. Evidence of tin oxide recrystallization in opacified lead glazes. *Journal of the American Ceramic Society* 82(10): 2871-2875. DOI: 10.1111/j.1151-2916.1999.tb02170.x
- Molera, J., Pradell, T., Salvadó, N., Vendrell-Saz, M. 2001. Interactions between clay bodies and lead glazes. *Journal of the American Ceramic Society* 84(5): 1120-1128. DOI: 10.1111/j.1151-2916.2001.tb00799.x
- Molera, J., Pradell, T., Salvado, N., Vendrell-Saz, M. 2009. Lead frits

- in Islamic and Hispano-Moresque glazed productions In: Shortland, A., Freestone, I., Rehren, Th. (Eds.) *From Mine to Microscope. Advances in the study of Ancient materials*. Chapter 1. Oxbow books, pp. 1-11.
- Molera, J., Coll, J., Labrador, A., Pradell, T. 2013. Manganese brown decorations in 10th to 18th century Spanish tin glazed ceramics. *Applied Clay Sciences* **82**: 86-90.
- Molera, J., Martinez Ferreras, V., Fusaro, A., Gurt Esparraguera, J.M., Gaudenzi, M., Pidaev, S.R., Pradell, T. (2020) Islamic glazed wares from ancient Termez (southern Uzbekistan). Raw materials and techniques. *Journal of Archaeological Science Reports*: 102169. DOI: 10.1016/j.jasrep.2019.102169
- Pace, M., Bianco Prevot, A., Mirti, P., Venco Ricciardi, R. (2008) The technology of production of Sasanian glazed pottery from Veh Ardašir (central Iraq). *Archaeometry* **50**(4): 591-605. DOI: 10.1111/j.1475-4754.2007.00369.x
- Pitskhelauri, K. 1973. *The problems for the Eastern Georgian Tribes in the XV-VII centuries BC*. Tbilisi [in Georgian].
- Pitskhelauri, K. 2005. *Central Transcaucasian Archaeological culture in the XIV-XIII centuries BC*. Tbilisi. [in Georgian]
- Popkhadze, N., Beridze, T., Moritz, R., Gugushvili, V., Khutsishvili, S. 2009. Facies analysis of the volcano-sedimentary host rocks of the Cretaceous Madneuli massive sulphide deposit, Bolnisi District, Georgia. *Bulletin of the Georgian National Academy of Sciences* **3**: 103-108.
- Rezesidze, N. 2011. The settlements of Late Bronze-Early Iron Age from Dmanisi. Georgian National Museum publishing house. Moambe II. (47-B). Tbilisi.
- Sagona, A.G. 2018. *The Archaeology of the Caucasus: From Earliest Settlements to the Iron Age*. Cambridge University Press.
- Salinas E, Pradell T (2018) The transition from lead transparent to tin-opacified glaze productions in the western Islamic lands: al-Andalus, c. 875–929 CE. *Journal of Archaeological Science* **94**: 1–11.
- Schillinger, A. 1997. *Die früheste Zinnbronze im Schwarzmeerraum*. Magisterarbeit, Universität Tübingen.
- Shaar, R., Tauxe, L., Goguitchaichvili, A., Devidze, M. and Licheli, V. 2017. Further evidence of the Levantine Iron Age geomagnetic anomaly from Georgian pottery. *Geophysical Research Letters*, **44**:2229-2236.
- Shepard, F.P. 1954. Nomenclature based on sand-silt-clay ratios. *Journal of Sedimentary Petrology* **24**:151-158. DOI: 10.1306/D4269774-2B26-11D7-8648000102C1865D
- Sokhadze, G., Floyd, M., Godoladze, T., King, R., Cowgill, E.S., Javakhishvili, Z., Hahubia, G., Reilinger, R. 2018. Active convergence between the Lesser and Greater Caucasus in Georgia: Constraints on the tectonic evolution of the Lesser–Greater Caucasus continental collision. *Earth and Planetary Science Letters* **481**: 154–161.
- Stöllner, Th., Gambashidze, I. 2014. The Gold Mine of Sakdrisi and early Mining and Metallurgy in Transcaucasus and the Kura-Valley System. In: Narimanishvili, G., Kvachadze, M., Puturidze, M.,

- Shanshashvili, N. (Eds.) *Problems of Early Metal Age Archaeology of Caucasus and Anatolia*. Proceedings of the International Conference (November 19-23, 2014), Tbilisi, pp. 101-124.
- Ting, C., Vionis, A., Rehren, Th., Kassianidou, V., Cook, H., Barker, C. (2019a) The beginning of glazed ware production in late medieval Cyprus. *Journal of Archaeological Science: Reports* **27**: 101963. DOI: 10.1016/j.jasrep.2019.101963
- Ting, C., Lichtenberger, A., Raja, A. (2019b) The technology and production of glazed ceramics from middle islamic Jerash, Jordan. *Archaeometry* **61**(6): 1296-1312. DOI: 10.1111/arc.12489
- Tite, M.S., Freestone, I.C., Mason, R., Molera, J., Vendrell-Saz, M., Wood, N. 1998. Lead glazes in Antiquity - Methods of production and reasons for use. *Archaeometry* **40**(2): 241-260. DOI: 10.1111/j.1475-4754.1998.tb00836.x
- Tite, M.S., Pradell, T., Shortland, A. 2008. Discovery, production and use of tin-based opacifiers in glasses, enamels and glazes from the Late Iron Age onwards: a reassessment. *Archaeometry* **50**(1): 67-84. DOI: 10.1111/j.1475-4754.2007.00339.x
- Trojsi, G., Positano, M., Palumbi, G., Di Lorenzo, A. 2002. Archaeometrical issues related to Transcaucasian pottery from Georgia. *Periodico di Mineralogia*, **71**:239-246.
- Tushishvili, N. 1972. *Madnischalis Cemetery*. Tbilisi. [in Georgian]
- von Suchodoletz, H., Gärtner, A., Hoth, S., Umlauf, J., Sukhishvili, L., Faust, D. 2016. Late Pleistocene river migrations in response to thrust belt advance and sediment-flux steering — The Kura River (southern Caucasus). *Geomorphology* **266**: 53–65.
- Yilmaz, A., Adamia, Sh., Chabukiani, A., Chkhotua, T., Erdogan, K., Tuzcu, S., Karabilykoglu, M., 2000. Structural correlation of the southern Transcaucasus (Georgia)-eastern Pontides (Turkey). In: Bozkurt, E., Winchester, J.A., Piper, J.D.A. (eds.), *Tectonics and magmatism in Turkey and the surrounding area*. Geological Society. London, Special Publication 173, pp. 171-182.
- Wilkinson, Ch.K. 1961. The Glazed Pottery of Nishapur and Samarkand. The Metropolitan Museum Art Bulletin. New York.
- Wilkinson, Ch.K. 1973. Nishapur: Pottery of the Early Islamic Period. New York.